HHS Public Access

Author manuscript

Photochem Photobiol. Author manuscript; available in PMC 2025 January 01.

Published in final edited form as:

Photochem Photobiol. 2024 ; 100(1): 67–74. doi:10.1111/php.13814.

Caged luciferins enable rapid multicomponent bioluminescence imaging

Mariana X. Navarro[1], **Caroline K. Brennan**[1], **Anna C. Love**[1], **Jennifer A. Prescher**[*,1,2,3]

[1]Department of Chemistry, University of California, Irvine 1120 Natural Science II, Irvine, CA 92617 (USA)

[2]Department of Molecular Biology and Biochemistry, University of California, Irvine, 3205 McGaugh Hall, Irvine, CA 92716 (USA)

[3]Department of Pharmaceutical Sciences, University of California, Irvine, 101 Theory, Suite 100, Irvine, CA 92617 (USA)

Abstract

Bioluminescence is a sensitive technique for imaging biological features over time. Historically, though, the modality has been challenging to employ for multiplexed tracking due to a lack of resolvable luciferase–luciferin pairs. Recent years have seen the development of numerous orthogonal probes for multi-parameter imaging. While successful, generating such tools often requires complex syntheses and lengthy enzyme evolution campaigns. This work showcases an alternative strategy for multiplexed bioluminescence that takes advantage of already-orthogonal caged luciferins and established uncaging enzymes. These probes generate unique bioluminescent signals that can be distinguished via a linear unmixing algorithm. Caged luciferins enabled two- and three-component imaging on the minutes time scale. We further showed that the tools can be used in conjunction with endogenous enzymes for multiplexed studies. Collectively, this approach lowers the barrier to multicomponent bioluminescence imaging and can be readily adopted by the broader community.

Graphical Abstract

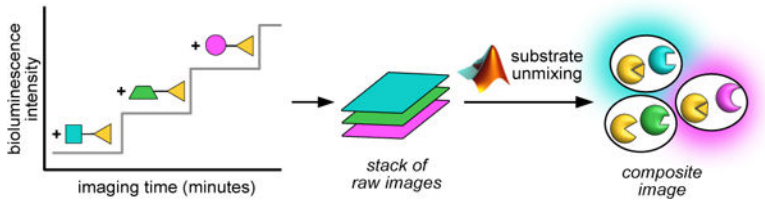

Unique luciferase-luciferin pairs are required for multiplexed bioluminescence imaging, but often require time- and labor-intensive processes to identify. In this work, we demonstrate that readily available caged luciferins and uncaging enzymes can be integrated into multicomponent

*Corresponding author: jpresche@uci.edu (Jennifer A. Prescher).

SUPPORTING INFORMATION

Additional supporting information may be found online in the Supporting Information section at the end of the article:

visualization schemes. Such already orthogonal probes broaden the scope and accessibility of bioluminescence imaging.

INTRODUCTION

Bioluminescence is a powerful imaging tool for visualizing cellular and molecular features (1). This technology relies on the oxidation of luciferin small molecules by luciferase enzymes to produce photons (2–4). Since bioluminescent probes do not require excitation light for detection, they can be advantageous for sensitive imaging studies (5). Indeed, luciferase–luciferin pairs are routinely used for monitoring cell proliferation, gene expression, and other parameters both in vitro and in vivo (6, 7). Most applications, though, have been limited to monitoring one feature at a time. Few bioluminescent probes are readily distinguishable via conventional spectral resolution methods. Consequently, multicomponent imaging remains challenging (8).

We and others have been addressing the need for expanded bioluminescence capabilities by developing resolvable luciferase–luciferin pairs (9–14). Several approaches have focused on enhancing spectral resolution, in which the imaging agents are separated by color (15–17). In a recent example, the Mezzanotte group and Promega Corporation engineered red-emitting luciferase–luciferin probes that could be resolved via spectral unmixing (18). Additional multiplexing is possible with the development of near-infrared bioluminescent tools (19). However, separating bioluminescent emitters by wavelength alone is often challenging, given the impacts of tissue on light propagation and conventional surface detection methods (20). Popular luciferases for in vivo imaging also harbor broad, overlapping spectra, complicating their discrimination. Therefore, many experiments require signal from one bioluminescent probe set to clear before a second luciferin is added, often requiring multiple hours—if not days—to complete.

An alternative strategy for multicomponent bioluminescence imaging exploits substrate resolution. Many luciferases exhibit distinct patterns of luciferin use, and several engineered enzymes have been developed that are responsive to designer luciferin analogs (orthogonal pairs, Figure 1a) (21–24). Differences in substrate use can be used to deconvolute combinations of luciferases via linear unmixing algorithms. This approach has been used to identify many combinations of both engineered and naturally orthogonal probes (25–27), and can be performed in a rapid manner via luciferin “layering” (9). No wait time is necessary for substrate clearance, prior to the addition of a new luciferin. Thus, luciferase reporters can be assigned via their patterns of emission with various substrates, in the span of minutes—a significant improvement over conventional imaging protocols. Like spectral separation, substrate unmixing can be used to successfully identify mixed populations of bioluminescent reporters (e.g., cells) in vivo (9).

Key to the success of multicomponent bioluminescence via substrate resolution is the identification of viable orthogonal pairs. Parallel engineering of luciferases and luciferins, while effective, typically requires cumbersome syntheses and extensive enzyme engineering efforts. For example, AkaLumine and Akaluc comprise a red-emitting probe set for deep tissue imaging (18, 28, 29). AkaLumine required a 5-step synthesis from hydroquinone

and an aromatic nitrile (24, 28). The matching enzyme, Akaluc, was uncovered after >20 rounds of directed evolution and comprises twenty-eight mutations (29). Such time- and labor-intensive procedures have hindered the rapid identification of additional useful probes.

We surmised that orthogonal luciferase–luciferin pairs could be more readily derived from existing and well-vetted molecular probes. We were specifically attracted to "caged" luciferins as already-orthogonal small molecules. These analogs comprise functional groups that block activity with the luciferase enzyme. In the presence of the corresponding "uncaging" biomolecule or enzyme, the luciferin scaffold is released and available for the luciferase reaction, enabling a bioluminescent readout. Light emission thus correlates with activity of the uncaging enzyme or activating biomolecule in the cellular environment. Caged probes have been used extensively in conjunction with firefly luciferase (Fluc) and its native substrate, D-luciferin (D-luc) (30–33) for in vitro and in vivo imaging. Caged D-luc scaffolds have been crafted to report on numerous enzymes, including cytochrome P450 (34) and caspase 3 (35), in addition to biomolecules and metal ions (30, 31). We aimed to leverage this vast collection for multiplexed imaging. The modularity of this approach would broaden the scope of accessibility of multiplexed, multicomponent imaging and potentially take advantage of endogenous enzyme activity.

MATERIALS AND METHODS

General cloning methods

Polymerase chain reaction (PCR) was performed to amplify genes of interest. mNeptune (36), nitroreductase (NTR) (37), blue fluorescent protein (BFP) (36), Firefly luciferase (Fluc) (*luc2*) (36), and green fluorescent protein (GFP) (36) genes were amplified from previously reported constructs. Human FAAH was purchased as a gene block from Genewiz©. pcDNA vector was used from plasmid pHM830, which was a gift from Thomas Stamminger (Addgene plasmid # 20702; http://n2t.net/addgene:20702; RRID:Addgene_20702). Primer melting temperatures were calculated using a melting temperature (T_m) calculator offered by New England BioLabs (https://tmcalculator.neb.com). All PCR reactions were performed using a BioRad C3000 Thermocycler using the following conditions: 1x Q5 Hot start DNA polymerase reaction buffer, dNTPs (0.8 mM), and Q5 Hot start DNA polymerase (1 U) in a total reaction volume of 50 μL, unless otherwise stated. The following thermal cycling conditions were used to amplify all inserts: initial denaturation at 95 ˚C for 180 s; 20 cycles of denaturation (95 ˚C, 30 s), annealing (72 ˚C over 30 s, −1.2 °C/cycle); 20 cycles of denaturation (95 ˚C, 30 s), annealing (60 ˚C over 30 s) and extension (72 ˚C, 180 s (FAAH) or 90 s (mNeptune, NTR, BFP, GFP, Fluc)). The PCR products were purified via gel electrophoresis using 1% agarose gels and products were identified using GelRed® Nucleic Acid Gel Stain (Fisher Scientific).

The inserts were assembled into a vector for mammalian cell transfection (pcDNA3.1). Plasmids were digested with *EcoR*I and *Hind*III (New England BioLabs) for 3 h at 37 ˚C. The products were purified from remaining circular template via gel electrophoresis in 1% agarose gels.

Inserts were assembled with linearized vectors using Gibson assembly (38). Gibson assembly master mixes were prepared following the recipe from Prather and coworkers (http://www.openwetware.org/wiki/Gibson_Assembly), with all materials purchased from New England BioLabs. For the assembly, 50 ng of linearized vector was combined with insert (2:1 insert:vector ratio) and added to 10 μL of master mix. The mixtures were incubated at 50˚C for 1 h, then transformed. Ligated plasmids were transformed into the TOP10 strain of *E. coli* using the heat shock method.

Primer lists

All primers were purchased from Integrated DNA Technologies, Inc. (San Diego, CA) and are written in the 5′ ⟶ 3′ direction (See Supporting Information, Table S1).

General bioluminescence imaging

Bioluminescence assays were performed in black 96-well plates (Grenier Bio-One). Plates containing luminescent reagents were imaged in a light-proof chamber with an IVIS Lumina (Xenogen) CCD camera chilled to –90 ˚C. The stage was kept at 37 ˚C during the imaging session and the camera was controlled using LivingImage software (version 4.3.1). Exposure times were set to 1–10 min and data binning levels were set to medium. Bioluminescence intensity values (photons/s) for regions of interest were analyzed using LivingImage software (version 4.3.1). Measurements were acquired in triplicate unless otherwise stated, and the data were analyzed using GraphPad Prism (version 9.1.2 for Macintosh, GraphPad Software).

Mammalian cell culture

HeLa (ATCC) and HEK293 cells (ATCC) were cultured in DMEM (Corning) supplemented with 10% (v/v) fetal bovine serum (FBS, Life Technologies), penicillin (100 U/mL), and streptomycin (100 μg/mL). Cells were maintained in a 5% (v/v) CO_2 water-saturated incubator at 37°C.

HeLa cells were transiently transfected with FAAH-mNeptune, NTR-BFP, β-gal-GFP, or luc2-IRES-GFP encoding constructs using cationic lipid formulations (Lipofectamine 3000; Invitrogen) according to manufacturer's instructions. Cells (1×10^5) were analyzed for expression with a NovoCyte Quanteon Flow Cytometer and used for imaging analysis 24 h post transfection (see Figure S5 for representative plots).

Bioluminescence imaging with mammalian cells

HeLa cells transiently expressing FAAH, NTR, β-gal, or Fluc (1×10^5 cells/well, 100 μL total volume) were plated immediately prior to imaging. A solution of each luciferin analog in 100 mM phosphate buffer (100 μL, 100 μM final concentration) was added to cells expressing either NTR/Fluc, β-gal/Fluc, FAAH/Fluc, or Fluc only. Cells were incubated for either 5 min (Lugal, D-luciferin amide) or 10 min (Luntr) prior to imaging (see Supporting Information, Figure S1). For rapid, multicomponent imaging experiments, the luciferins were sequentially added to the cell populations of interest. For example, as shown in Figure 3, Luntr was incubated for 10 min with cells expressing NTR/Fluc, β-gal/Fluc, or FAAH/Fluc. After an image was acquired, Lugal was added to the same cell populations, and an

image was acquired after 5 min. Finally, D-luciferin amide was added to the cell samples, and a third image was acquired after 5 min. The images were and analyzed as described above.

Substrate unmixing

Substrate unmixing experiments were designed as previously described (36). *SubstrateUnmixing* was conducted with MATLAB R2020a. Luminescence images containing the raw CCD counts (as TIFF files) were loaded into MATLAB. Images were subjected to a 2-pixel median filter (using the *medfilt2* function with a 5×5 neighborhood around the corresponding pixel). Next, the signal at each pixel was normalized to lie between 0 and 65536 (the maximum value that can be stored in a 16-bit image). As a result, the brightest pixel in each image had a value of 65536, and the dimmest had a value of 0. Regions of interest were generated by identifying the image coordinate of the reference well and input dimensions. Once assigned, the MATLAB algorithm was run to perform the unmixing. After unmixing, text images were imported into ImageJ (installed under the FIJI package). Integrated pixel values for regions of interest were analyzed using the “Measure” tool. Psuedocolors were assigned with the “Merge Channels” tool.

Imaging cell mixtures via substrate unmixing

Cells were plated such that 2×10^4 expressing cells were present in the reference wells, 1×10^4 expressing cells were present in the 1x wells and 5×10^4 expressing cells were present in the 5x wells. The numbers of expressing cells were calculated from flow cytometry analyses of cells transfected with the corresponding uncaging enzyme and Fluc constructs. Small molecule luciferins were added and imaged as described above.

General synthetic information

All reagents and solvents were purchased from commercial suppliers and used as received. Appel’s salt, 4,5-dichloro-1,2,3-dithiazolium chloride (6) was either purchased from LabNetwork (CAS #: 75318–43-3) or prepared according to literature precedent (39–41). Lugal, D-luciferin-6-O β-D-galactopyranoside, was purchased from Biosynth Carbosynth® (CAS #: 131474–38-9). Compounds **1–5** were prepared according to literature precedent (32, 42).

RESULTS AND DISCUSSION

We hypothesized that caged luciferins and their corresponding uncaging enzymes would interface with the rapid linear unmixing algorithm developed previously in our lab, streamlining multicomponent imaging (9, 36). Only in the presence of cells expressing both the corresponding uncaging enzyme and Fluc, would bioluminescent signal be produced upon incubation of the corresponding caged luciferin (Figure 1b). Distinct patterns of light emission (in terms of output intensity of each small molecule paired with each uncaging enzyme) would correlate with defined imaging targets, enabling their rapid discrimination (cartoon depiction shown in Figure 1b) (22, 36).

To achieve multicomponent bioluminescence imaging with caged luciferins and their corresponding activating enzymes, we leveraged well-known probes: Luntr (42), Lugal (33, 43), and D-luciferin amide (32). Luntr and Lugal comprise cages at the C6′ position of D-luc, masking the native hydroxy group (Figure 2a). This moiety is essential to the light-emitting bioluminescent reaction. Luntr features a nitro group that is uncaged by nitroreductase (NTR). This uncaging reaction yields a hydroxylamine or amine substituent, restoring electron-donating character at C6′, a necessary feature for light emission (42). NTR is widely used to activate prodrugs and fluorophores in vitro and in vivo (44–50), as it is absent in mammalian cells. Lugal comprises a galactose cage at the C6′ position; this group is selectively removed by β-galactosidase (β-gal) (51). Galactose cages/β-gal have also been widely used in biological studies (33, 52).

The remaining analog, D-luciferin amide, features an amide at the C4 position of the luciferin scaffold. This group masks the requisite carboxyl group used in the light-emitting bioluminescent reaction. The amide can be removed by fatty acid amide hydrolase (FAAH). FAAH is responsible for the hydrolysis of bioactive lipids, fatty acid amides (FAA), to their fatty acid counterparts (53). FAAH is overexpressed in cancer cells and has elevated expression in the brain (54). In recent work, Miller and coworkers capitalized on this differential expression to image FAAH activity in brain tissue (32). D-Luciferin amide was synthesized and used to illuminate FAAH levels in vivo (10). With the amide cage in place, no light emission was observed; FAAH activity released the activated luciferin, which could be detected in luciferase-expressing tissues in vivo.

To evaluate caged luciferins in the context of multicomponent imaging, we performed initial cell assays with uncaging enzymes. HeLa cells expressing either β-gal, NTR, or FAAH, in addition to Fluc, were treated with the caged substrates (Figure 2b). Compounds were added at 100 μM final concentration and light emission was measured after 5–10 min of incubation (see Supporting Information, Figure S1). Minimal background signal from non-specific degradation of the caged luciferins was observed (See Supporting Information, Figure S1). D-Luciferin amide provided the most robust signal enhancement (220-fold and 178-fold increase in output in FAAH/Fluc expressing cells compared to NTR/Fluc and β-gal/Fluc expressing cells, respectively). Luntr also provided robust signal upon incubation with NTR-expressing cells (50-fold signal increase in output in β-gal/Fluc expressing cells).

Compared to other samples, Lugal provided significant light output with its matched uncaging enzyme (β-gal), but the signal enhancements were less pronounced (2–7-fold). Inflated background signal from FAAH/Fluc and NTR/Fluc expressing cells was attributed to the endogenous expression of β-gal by HeLa cells (54), leading to non-specific Lugal uncaging, although other routes of degradation are possible. Regardless of the mechanism, off-target uncaging is not completely detrimental to the approach, though, as the distinct patterns of light emission (instead of total output intensity) observed with all three substrates can be unmixed (9, 36). That is, even though the measured outputs do not show perfect orthogonality, the uncaging enzymes and substrate pairs are still distinguishable.

After establishing the preferential uncaging of the luciferin analogs, we next assessed whether the probes could be used for rapid multicomponent imaging. HeLa cells expressing

NTR, β-gal, or FAAH, in addition to Fluc, were plated in separate wells (Figure 3a). We added each of the caged probes in rapid succession. Based on previous work (36), the luciferin analogs were added in order of dimmest probe to brightest: Luntr, then Lugal, and last, D-luciferin amide. The total imaging time required via this strategy was ~35 minutes, a vast improvement over traditional approaches that require signal diminishment from one small molecule-luciferin pair prior to addition of the subsequent luciferin. After imaging, we used the linear unmixing algorithm, named *SubstrateUnmixing* (36) to deconvolute the specific substrate signatures. The patterns of light emission were then assigned false colors. As shown in Figure 3b, the unmixing algorithm readily identified the distinct populations of cells expressing either NTR, β-gal, or FAAH. Incubation and imaging of Luntr uncaging and turnover by Fluc yielded on average a 47-fold signal induction over β-gal- and FAAH-expressing cells. The addition of Lugal yielded a 6-fold signal induction in β-gal-expressing cells over NTR- or FAAH-expressing cells, while addition of D-luciferin amide demonstrated a 131-fold signal induction over NTR- or β-gal-expressing cells (Figure 3c). Interestingly, the intensity of light produced upon addition of Lugal or Luntr was similar in the multicomponent assay. The overall patterns of light emission remained distinct, though, enabling successful unmixing. It was also possible to reverse the order of addition (Lugal first, then Luntr, then D-luciferin amide) and unmix the signals (See Supporting Information, Figure S2a–c).

Once we established that classic uncaging enzymes are suitable for rapid, multicomponent bioluminescence imaging, we applied the workflow to another biologically relevant model. Many well-known uncaging enzymes are endogenously expressed by bacteria and other cell types, suggesting that they can be directly integrated into multicomponent experiments. FAAH/Fluc- and β-gal/Fluc-expressing HeLa cells were plated together with Fluc-expressing bacteria that naturally produce NTR (See Supporting Information, Figure S3a). We hypothesized that endogenous NTR would be sufficient to uncage Luntr, setting the stage for studies of host–microbe interactions. After administration of all three caged luciferins, the raw bioluminescent images were successfully unmixed (See Supporting Information, Figure S3b–c). These data indicate that the imaging approach can be used in conjunction with cells expressing endogenous enzymes for which corresponding caged luciferins exist.

Complex mixtures of cells were also amenable to imaging via sequential addition and linear unmixing of caged luciferins. Cell mixtures containing NTR/Fluc- and FAAH/Fluc-expressing cells were plated at ratios of 1:1, 5:1, or 1:5 of NTR:FAAH expressing cells (Figure 4a). Populations comprising a single cell type were also plated as reference wells for linear unmixing (Figure 4a). The cells were treated sequentially with the caged luciferins and imaged. The bioluminescent images were then unmixed and false colored (Figure 4b–c). Mixtures comprising more of one cell type than another were successfully identified (Figure 4d). Mixtures of Lugal/Fluc- and FAAH/Fluc-expressing cells were similarly successfully imaged and unmixed (See Supporting Information, Figure S4a–c).

In conclusion, we showed that caged luciferins can be repurposed as multiplexed imaging tools. This novel approach to multicomponent bioluminescence enables a broad range of studies with widely accessible probes. We also showed that the imaging technique

is compatible with endogenous uncaging enzymes, such as NTR expressed in bacteria. These results set the stage for additional multicomponent imaging with cells and organisms often used in conjunction with caged luciferins. While enabling new studies, the approach reported here is not without limitation. The method requires serial application of multiple substrates in a single imaging session, a feature that can be limiting for capturing certain dynamic processes. Premature uncaging of the luciferin analogs can also reduce the imaging sensitivity. New designer probes (55) and improved methods for rapid delivery will help to address these shortcomings, and broaden the utility of multicomponent bioluminescence via substrate unmixing.

Supplementary Material

Refer to Web version on PubMed Central for supplementary material.

ACKNOWLEDGMENTS:

This work was supported by the U.S. National Institutes of Health (R01 GM107630) and the University of California, Irvine (UCI) School of Physical Sciences. M.X.N was supported by the National Science Foundation Graduate Research Fellowship under Grant No. DGE-1839285. C. B. K. was supported by the UCI Physical Sciences Machine Learning NEXUS program. We thank members of the Prescher laboratory for experimental advice and helpful discussions.

REFERENCES

1. Kaskova ZM, Tsarkova AS and Yampolsky IV (2016) 1001 Lights: Luciferins, Luciferases, Their Mechanisms of Action and Applications in Chemical Analysis, Biology and Medicine. Chem. Soc. Rev 45, 6048–6077. [PubMed: 27711774]
2. Syed AJ and Anderson JC (2021) Applications of Bioluminescence in Biotechnology and Beyond. Chem. Soc. Rev 50, 5668–5705. [PubMed: 33735357]
3. Fleiss A and Sarkisyan KS (2019) A Brief Review of Bioluminescent Systems. Curr. Genet. 65, 877–882. [PubMed: 30850867]
4. Prescher JA and Contag CH (2010) Guided by the Light: Visualizing Biomolecular Processes in Living Animals with Bioluminescence. Curr. Opin. Chem. Biol 14, 80–89. [PubMed: 19962933]
5. Mezzanotte L, van ‘t Root M, Karatas H, Goun EA and Löwik CWGM (2017) In Vivo Molecular Bioluminescence Imaging: New Tools and Applications. Trends Biotechnol 35, 640–652. [PubMed: 28501458]
6. Sellmyer MA, Richman SA, Lohith K, Hou C, Weng C-C, Mach RH, O’Connor RS, Milone MC and Farwell MD (2020) Imaging CAR T Cell Trafficking with EDHFR as a PET Reporter Gene. Mol. Ther 28, 42–51. [PubMed: 31668558]
7. Bhaumik S and Gambhir SS, (2002) Optical Imaging of Renilla Luciferase Reporter Gene Expression in Living Mice. Proc. Natl. Acad. Sci. U. S. A 99, 377–382. [PubMed: 11752410]
8. Zambito G, Chawda C and Mezzanotte L, (2021) Emerging Tools for Bioluminescence Imaging. Curr. Opin. Chem. Biol 63, 86–94. [PubMed: 33770744]
9. Rathbun CM, Ionkina AA, Yao Z, Jones KA, Porterfield WB and Prescher JA (2021) Rapid Multicomponent Bioluminescence Imaging via Substrate Unmixing. ACS Chem. Biol 16, 682–690. [PubMed: 33729750]
10. Rumyantsev KA, Turoverov KK and Verkhusha VV (2016) Near-Infrared Bioluminescent Proteins for Two-Color Multimodal Imaging. Sci. Rep 6, 36588. [PubMed: 27833162]
11. Aswendt M, Vogel S, Schäfer C, Jathoul A, Pule M and Hoehn M (2019) Quantitative in Vivo Dual-Color Bioluminescence Imaging in the Mouse Brain. Neurophotonics 6, 025006. [PubMed: 31093514]

12. Gammon ST, Leevy WM, Gross S, Gokel GW and Piwnica-Worms D (2006) Spectral Unmixing of Multicolored Bioluminescence Emitted from Heterogeneous Biological Sources. Anal. Chem 78, 1520–1527. [PubMed: 16503603]
13. Zambito G, Mishra G, Schliehe C and Mezzanotte L (2022) Near-Infrared Bioluminescence Imaging of Macrophage Sensors for Cancer Detection In Vivo. Front. Bioeng. Biotechnol 10, 867164. [PubMed: 35615475]
14. Yao Z, Brennan CK, Scipioni L, Chen H, Ng KK, Tedeschi G, Parag-Sharma K, Amelio AL, Gratton E, Digman MA and Prescher JA (2022) Multiplexed Bioluminescence Microscopy via Phasor Analysis. Nat. Methods 19, 893–898. [PubMed: 35739310]
15. Jathoul AP, Grounds D, Anderson JC and Pule MA (2014) A Dual-Color Far-Red to Near-Infrared Firefly Luciferin Analogue Designed for Multiparametric Bioluminescence Imaging. Angew. Chem., Int. Ed 53, 13059–13063.
16. Stowe CL, Burley TA, Allan H, Vinci M, Kramer-Marek G, Ciobota DM, Parkinson GN, Southworth TL, Agliardi G, Hotblack A, Lythgoe MF, Branchini BR, Kalber TL, Anderson JC and Pule MA (2019) Near-Infrared Dual Bioluminescence Imaging in Mouse Models of Cancer Using Infraluciferin. eLife 8, e45801. [PubMed: 31610848]
17. Jathoul AP, Branchini BR, Anderson JC and Murray JAH (2022) A Higher Spectral Range of Beetle Bioluminescence with Infraluciferin. Front. Bioeng. Biotechnol 10, 897272. [PubMed: 36091447]
18. Zambito G, Hall MP, Wood MG, Gaspar N, Ridwan Y, Stellari FF, Shi C, Kirkland TA, Encell LP, Löwik C and Mezzanotte L (2021) Red-Shifted Click Beetle Luciferase Mutant Expands the Multicolor Bioluminescent Palette for Deep Tissue Imaging. iScience 24, 101986. [PubMed: 33490896]
19. Tiwari DK, Tiwari M and Jin T (2020) Near-Infrared Fluorescent Protein and Bioluminescence-Based Probes for High-Resolution in Vivo Optical Imaging. Mater. Adv 1, 967–987.
20. Mezzanotte L, Que I, Kaijzel E, Branchini B, Roda A, and Lowick C (2011) Sensitive Dual Color In Vivo Bioluminescence Imaging Using a New Red Codon Optimized Firefly Luciferase and a Green Click Beetle Luciferase. PLoS One 6, e19277. [PubMed: 21544210]
21. Hall MP, Unch J, Binkowski BF, Valley MP, Butler BL, Wood MG, Otto P, Zimmerman K, Vidugiris G, Machleidt T, Robers MB, Benink HA, Eggers CT, Slater MR, Meisenheimer PL, Klaubert DH, Fan F, Encell LP and Wood KV (2012) Engineered Luciferase Reporter from a Deep Sea Shrimp Utilizing a Novel Imidazopyrazinone Substrate. ACS Chem. Biol 7, 1848–1857. [PubMed: 22894855]
22. Williams SJ and Prescher JA (2019) Building Biological Flashlights: Orthogonal Luciferases and Luciferins for in Vivo Imaging. Acc. Chem. Res 52, 3039–3050. [PubMed: 31593431]
23. Jones KA, Porterfield WB, Rathbun CM, McCutcheon DC, Paley MA and Prescher JA (2017) Orthogonal Luciferase–Luciferin Pairs for Bioluminescence Imaging. J. Am. Chem. Soc 139, 2351–2358. [PubMed: 28106389]
24. Iwano S, Obata R, Miura C, Kiyama M, Hama K, Nakamura M, Amano Y, Kojima S, Hirano T, Maki S and Niwa H (2013) Development of Simple Firefly Luciferin Analogs Emitting Blue, Green, Red, and near-Infrared Biological Window Light. Tetrahedron 69, 3847–3856.
25. Williams SJ, Hwang CS and Prescher JA (2021) Orthogonal Bioluminescent Probes from Disubstituted Luciferins. Biochemistry 60, 563–572. [PubMed: 33599497]
26. Chien JC-Y, Badr CE and Lai CP-K (2021) Multiplexed Bioluminescence-Mediated Tracking of DNA Double-Strand Break Repairs in Vitro and in Vivo. Nat. Protoc 16, 3933–3953. [PubMed: 34163064]
27. Minegishi M, Kuchimaru T, Nakagawa K, Isozaki T, Fujimori S, Kadonosono T and Kizaka-Kondoh S (2021) Multiplexed Bioluminescence Imaging of Cancer Cell Response to Hypoxia and Inflammation in the Caudal-Artery Injection Model of Bone Metastasis during Zoledronic Acid Treatment. J. Cancer Metastasis Treat 7, 5.
28. Kuchimaru T, Iwano S, Kiyama M, Mitsumata S, Kadonosono T, Niwa H, Maki S and Kizaka-Kondoh S (2016) A Luciferin Analogue Generating Near-Infrared Bioluminescence Achieves Highly Sensitive Deep-Tissue Imaging. Nat. Commun 7, 11856. [PubMed: 27297211]

29. Iwano S, Sugiyama M, Hama H, Watakabe A, Hasegawa N, Kuchimaru T, Tanaka KZ, Takahashi M, Ishida Y, Hata J, Shimozono S, Namiki K, Fukano T, Kiyama M, Okano H, Kizaka-Kondoh S, McHugh TJ, Yamamori T, Hioki H, Maki S and Miyawaki A (2018) Single-Cell Bioluminescence Imaging of Deep Tissue in Freely Moving Animals. Science 359, 935–939. [PubMed: 29472486]
30. Su TA, Bruemmer KJ and Chang CJ (2019) Caged Luciferins for Bioluminescent Activity-Based Sensing. Curr. Opin. Biotechnol 60, 198–204. [PubMed: 31200275]
31. Li J, Chen L, Du L and Li M (2013) Cage the Firefly Luciferin! - A Strategy for Developing Bioluminescent Probes. Chem. Soc. Rev 42, 662–676. [PubMed: 23099531]
32. Mofford DM, Adams ST, Reddy GSKK, Reddy GR and Miller SC (2015) Luciferin Amides Enable in Vivo Bioluminescence Detection of Endogenous Fatty Acid Amide Hydrolase Activity. J. Am. Chem. Soc 137, 8684–8687. [PubMed: 26120870]
33. Wehrman TS, von Degenfeld G, Krutzik PO, Nolan GP and Blau HM (2006) Luminescent Imaging of β-Galactosidase Activity in Living Subjects Using Sequential Reporter-Enzyme Luminescence. Nat. Methods 3, 295–301. [PubMed: 16554835]
34. Meisenheimer PL, Uyeda HT, Ma D, Sobol M, McDougall MG, Corona C, Simpson D, Klaubert DH and Cali JJ (2011) Proluciferin Acetals as Bioluminogenic Substrates for Cytochrome P450 Activity and Probes for CYP3A Inhibition. Drug Metab. Dispos 39, 2403–2410. [PubMed: 21890735]
35. O'Brien MA, Daily WJ, Hesselberth PE, Moravec RA, Scurria MA, Klaubert DH, Bulleit RF and Wood KV (2005) Homogeneous, Bioluminescent Protease Assays: Caspase-3 as a Model. J. Biomol. Screen 10, 137–148. [PubMed: 15799957]
36. Brennan CK, Yao Z, Ionkina AA, Rathbun CM, Sathishkumar B and Prescher JA (2022) Multiplexed Bioluminescence Imaging with a Generalized Substrate Unmixing Algorithm. Cell Chem. Biol 29, 1649–1660. [PubMed: 36283402]
37. Gruber TD, Krishnamurthy C, Grimm JB, Tadross MR, Wysocki LM, Gartner ZJ and Lavis LD (2018) Cell-Specific Chemical Delivery Using a Selective Nitroreductase–Nitroaryl Pair. ACS Chem. Biol 13, 2888–2896. [PubMed: 30111097]
38. Gibson DG, Young L, Chuang R, Venter JC, Hutchison CA and Smith HO (2009) Enzymatic Assembly of DNA Molecules up to Several Hundred Kilobases. Nat. Methods 6, 343–345. [PubMed: 19363495]
39. McCutcheon DC, Paley MA, Steinhardt RC and Prescher JA (2012) Expedient Synthesis of Electronically Modified Luciferins for Bioluminescence Imaging. J. Am. Chem. Soc 134, 7604–7607. [PubMed: 22519459]
40. Appel R, Janssen H, Siray M and Knoch F (1985) Synthese und Reaktionen des 4,5-Dichlor-1,2,3-dithiazolium-chlorids. Chemische Berichte 118, 1632–1643.
41. English RF, Rakitin OA, Rees CW and Vlasova OG (1997) Conversion of Imino-1,2,3-Dithiazoles into 2-Cyanobenzothiazoles, Cyanoimidoyl Chlorides and Diatomic Sulfur. J. Am. Chem. Soc 0, 201–206.
42. Porterfield WB, Jones KA, McCutcheon DC and Prescher JA (2015) A "Caged" Luciferin for Imaging Cell–Cell Contacts. J. Am. Chem. Soc 137, 8656–8659. [PubMed: 26098396]
43. Geiger R, Schneider E, Wallenfels K and Miska W (1992) A New Ultrasensitive Bioluminogenic Enzyme Substrate for Beta-Galactosidase. Biol. Chem. Hoppe Seyler 373, 1187–1191. [PubMed: 1292503]
44. Wand ME, Taylor HV, Auer JL, Bock LJ, Hind CK, Jamshidi S, Rahman KM and Sutton JM (2019) Evaluating the Level of Nitroreductase Activity in Clinical Klebsiella Pneumoniae Isolates to Support Strategies for Nitro Drug and Prodrug Development. Int. J. Antimicrob. Agents 54, 538–546. [PubMed: 31398484]
45. Nagakubo D, Swann JB, Birmelin S and Boehm T (2017) Autoimmunity Associated with Chemically Induced Thymic Dysplasia. Int. Immunol 29, 385–390. [PubMed: 28992076]
46. Yamazoe S, McQuade LE and Chen JK (2014) Nitroreductase-Activatable Morpholino Oligonucleotides for in Vivo Gene Silencing. ACS Chem. Biol 9, 1985–1990. [PubMed: 25069083]
47. Herrlinger E-M, Hau M, Redhaber DM, Greve G, Willmann D, Steimle S, Mueller M, Luebbert M, Christoph C, Schuele R and Jung M (2020) Nitroreductase-Mediated Release of Inhibitors of

Lysine-Specific Demethylase 1 (LSD1) from Prodrugs in Transfected Acute Myeloid Leukaemia Cells. Chem. Bio. Chem 21, 2329–2347.

48. Searle PF, Chen M-J, Hu L, Race PR, Lovering AL, Grove JI, Guise C, Jaberipour M, James ND, Mautner V, Young LS, Kerr DJ, Mountain A, White SA and Hyde EI (2004) Nitroreductase: A Prodrug-Activating Enzyme for Cancer Gene Therapy. Clin. Exp. Pharmacol. Physiol 31, 811–816. [PubMed: 15566399]
49. Ji Y, Wang Y, Zhang N, Xu S, Zhang L, Wang Q, Zhang Q and Hu H-Y (2019) Cell-Permeable Fluorogenic Probes for Identification and Imaging Nitroreductases in Live Bacterial Cells. J. Org. Chem 84, 1299–1309. [PubMed: 30589544]
50. Hibbard HA and Reynolds MM (2019) Synthesis of Novel Nitroreductase Enzyme-Activated Nitric Oxide Prodrugs to Site-Specifically Kill Bacteria. Bioorg. Chem 93, 103318. [PubMed: 31586703]
51. Juers DH, Matthews BW and Huber RE (2012) LacZ β-Galactosidase: Structure and Function of an Enzyme of Historical and Molecular Biological Importance. Protein Sci 21, 1792–1807. [PubMed: 23011886]
52. Sharma SK and Leblanc RM (2017) Biosensors Based on β-Galactosidase Enzyme: Recent Advances and Perspectives. Anal. Biochem 535, 1–11. [PubMed: 28735682]
53. McKinney MK and Cravatt BF (2005) Structure and Function of Fatty Acid Amide Hydrolase. Annu. Rev. Biochem 74, 411–432. [PubMed: 15952893]
54. Uhlén M, Björling E, Agaton C, Szigyarto CA-K, Amini B, Andersen E, Andersson A-C, Angelidou P, Asplund A, Asplund C, Berglund L, Bergström K, Brumer H, Cerjan D, Ekström M, Elobeid A, Eriksson C, Fagerberg L, Falk R, Fall J, Forsberg M, Björklund MG, Gumbel K, Halimi A, Hallin I, Hamsten C, Hansson M, Hedhammar M, Hercules G, Kampf C, Larsson K, Lindskog M, Lodewyckx W, Lund J, Lundeberg J, Magnusson K, Malm E, Nilsson P, Ödling J, Oksvold P, Olsson I, Öster E, Ottosson J, Paavilainen L, Persson A, Rimini R, Rockberg J, Runeson M, Sivertsson Å, Sköllermo A, Steen J, Stenvall M, Sterky F, Strömberg S, Sundberg M, Tegel H, Tourle S, Wahlund E, Waldén A, Wan J, Wernérus H, Westberg J, Wester K, Wrethagen U, Xu LL, Hober S and Pontén F (2005) A Human Protein Atlas for Normal and Cancer Tissues Based on Antibody Proteomics. Mol. Cell. Proteom 4, 1920–1932.
55. Yadav AK, Zhao Z, Weng Y, Gardner SH, Brady CJ, Pichardo Peguero OD and Chan J (2023) Hydrolysis-Resistant Ester-Based Linkers for Development of Activity-Based NIR Bioluminescence Probes J. Am. Chem. Soc (in press, DOI: XXXXX.xxxxxx).

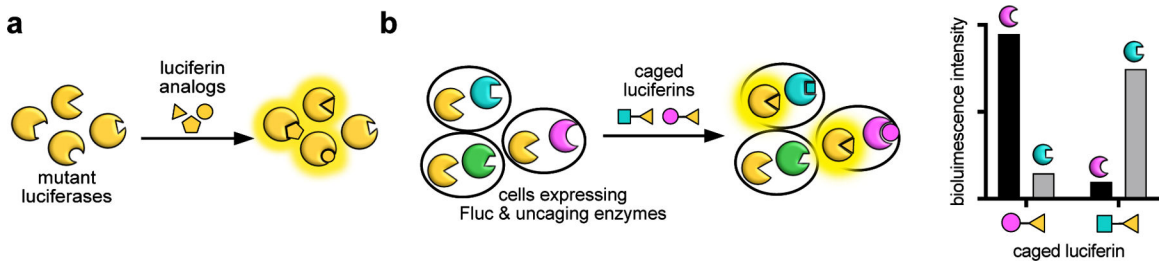

Figure 1.

Uncaging strategy employing caged luciferin probes for bioluminescent multicomponent imaging. (**a**) Previous strategy for developing luciferase–luciferin pairs through enzyme engineering and chemical modification. Mutant luciferase enzymes are depicted as enzymes with unique active sites that match corresponding small molecule luciferins. (**b**) Current strategy employing caged luciferin probes and distinct cell populations expressing Fluc and uncaging enzymes. A single luciferase enzyme (yellow) is expressed in each cell type, along with a unique uncaging enzyme (blue, magenta, or green). The uncaging enzymes liberate active luciferins, which are subsequently processed by Fluc to emit light. The accompanying cartoon graph shows an idealized reactivity pattern of caged luciferins in the presence of uncaging enzymes and Fluc. Each caged luciferin should be selectively uncaged with the corresponding enzyme, which in turn, produces a selective luminescent signal in the presence of Fluc.

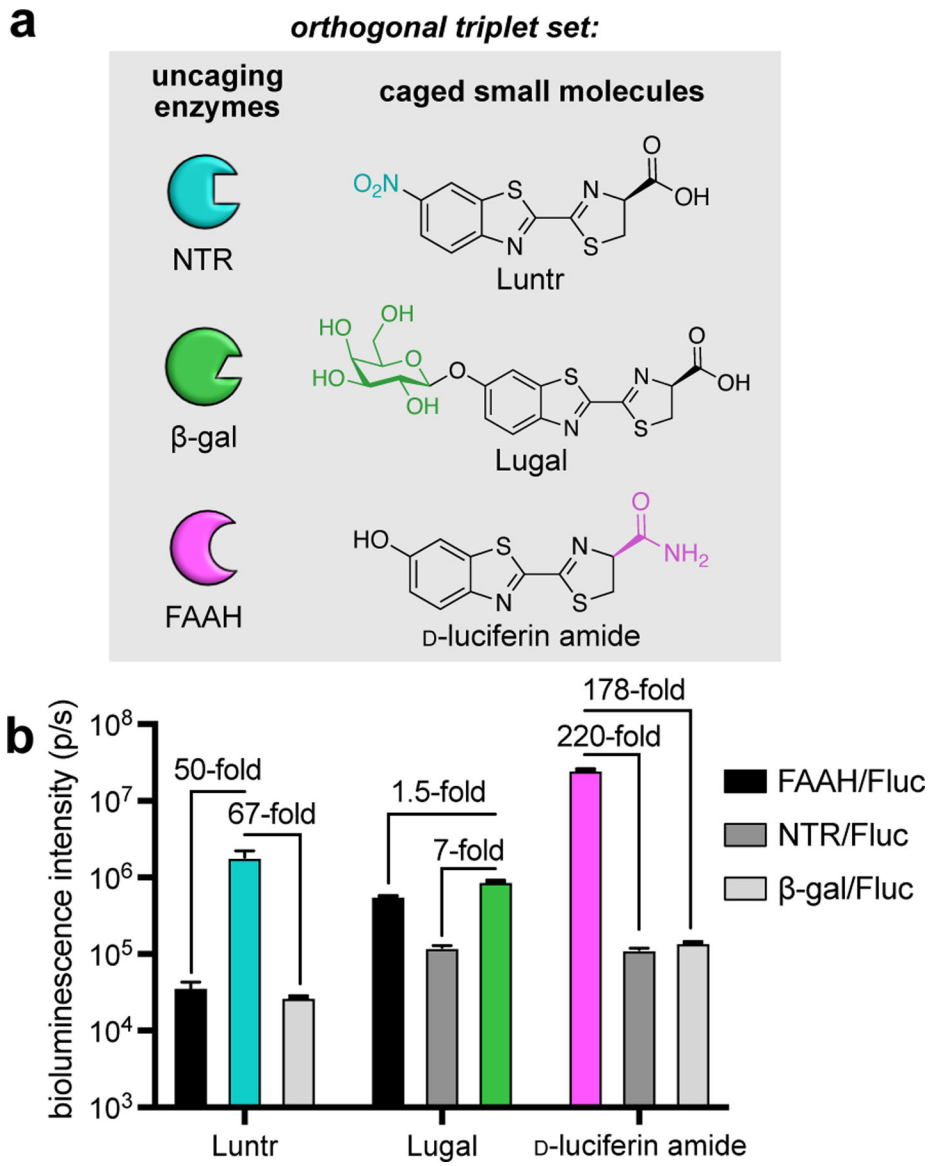

Figure 2.

Evaluating the robustness of caged luciferins as orthogonal probes. (**a**) Triplet set of caged luciferin/uncaging enzyme pairs evaluated in this work: Luntr/NTR, Lugal/β-gal, and D-luciferin amide/FAAH. (**b**) Singly-caged luciferins (100 μM) Luntr, Lugal, and D-luciferin amide were added to HeLa cells expressing either NTR/Fluc, β-gal/Fluc, or FAAH/Fluc and light output was evaluated after a 5–10 min incubation. Colored bars indicate the "matched" analogs and uncaging enzymes.

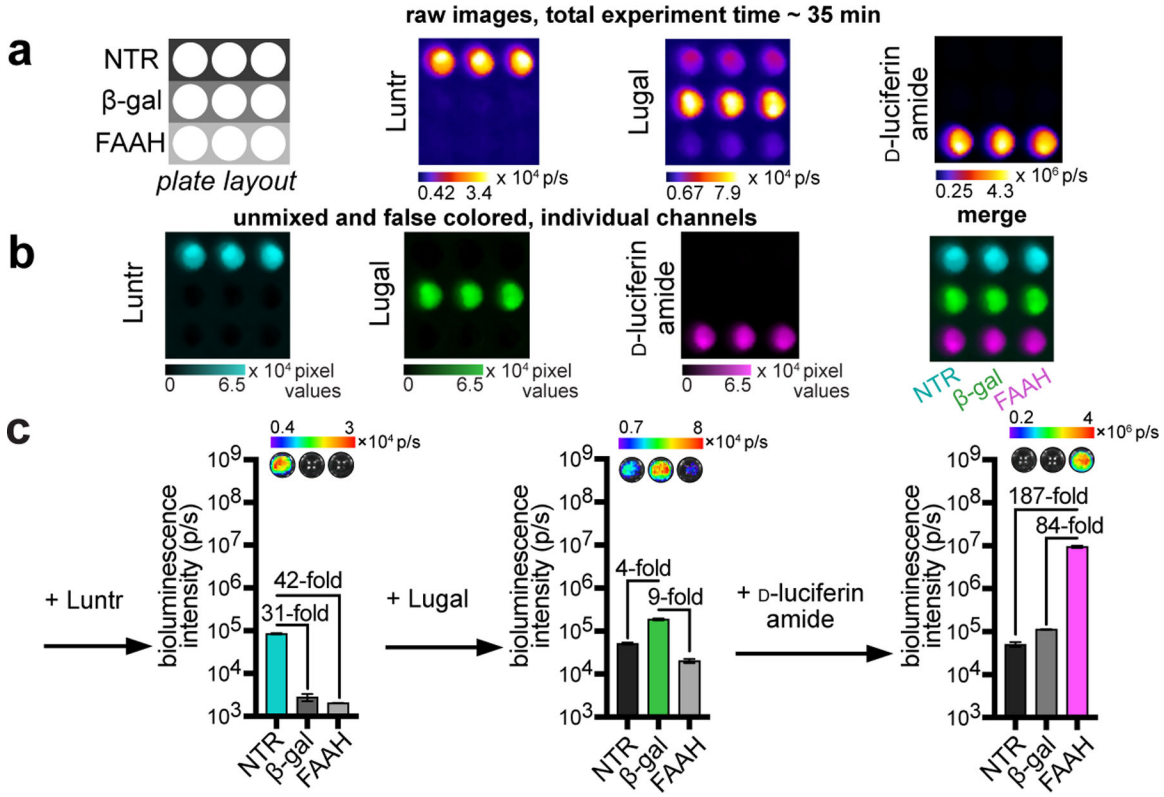

Figure 3.

Rapid imaging of luciferase mixtures using caged luciferins. Lugal, Luntr, and D-luciferin amide were added to HeLa cells expressing β-gal/Fluc, NTR/Fluc, and FAAH/Fluc. (**a**) Experimental set up and raw bioluminescence images after the addition of each luciferin analog (100 μM). (**b**) Unmixed and false colored images demonstrate multicomponent imaging with caged luciferin probes. (**c**) Bioluminescence intensity values from bioluminescent images with sequential addition of the small molecule luciferins.

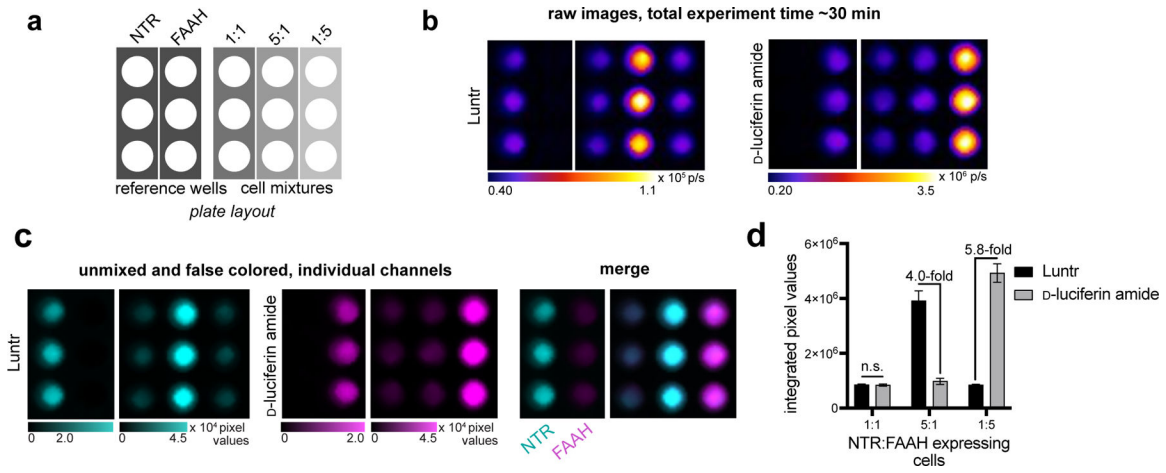

Figure 4.

Two-component BLI with varying cell mixtures. (**a**) Experimental layout for imaging mixtures of cells expressing Fluc in addition to cells expressing NTR or FAAH. Single populations of cells were also included as reference controls. (**b**) Multicomponent imaging of cell mixtures. Caged molecules Luntr and D-luciferin amide were added to all wells (100 μM) and raw images were collected after addition of each luciferin. (**c**) Images were unmixed and false colored. (**d**) Integrated pixel values from unmixed images were quantified.